Macromolecular Chemistry and Physics

Macromolecular Chemistry and Physics
www.mcp-journal.de

RESEARCH ARTICLE OPEN ACCESS

Synthesis of High Molecular Weight Isocyanate-Free Polyurethanes by Transurethanization of Dimethyl Carbamate With Mixtures of Long and Short Chain Diols

Nichollas G. Jaques[1,2] | Étienne Grau[1] | Audrey Llevot[1] | Thomas Vidil[1] | Michael A. R. Meier[2] | Henri Cramail[1]

[1]Univ. Bordeaux, Pessac, France | [2]Institute of Organic Chemistry (IOC) & Institute of Biological and Chemical Systems – Functional Molecular Systems (IBCS-FMS), Karlsruhe Institute of Technology, Karlsruhe, Germany

Correspondence: Michael A. R. Meier (m.a.r.meier@kit.edu) | Henri Cramail (henri.cramail@enscbp.fr)

Received: 27 April 2025 | **Revised:** 10 July 2025 | **Accepted:** 23 July 2025

Funding: The authors would like to express thanks for the financial support provided by the NIPU-EJD project; this project has received funding from the European Union's Horizon 2020 research and innovation program under Marie Skłodowska-Curie Grant Agreement No. 955700.

Keywords: carbamate | NIPU | polycondensation | poly(ether urethanes) | transurethanization

ABSTRACT

Due to sustainability challenges associated with conventional polyurethanes (PUs), non-isocyanate polyurethanes (NIPUs) synthesized via transurethanization of bismethylcarbamates and diols provide a more environmentally friendly alternative for thermoplastic PU production. In this study, NIPUs were synthesized by transurethanization of dimethyl dodecane-1,12-diyldicarbamate with one polyol dihydroxy-telechelic poly(ethylene glycol) and two short-chain diols (1,5-pentanediol and 1,12-dodecanediol). The reaction was optimized using dihydroxy-telechelic poly(ethylene glycol) as a model diol, where the choice of KO*t*Bu as a catalyst, a controlled alcohol/carbamate ratio (0.9) and mechanical stirring, enabled the production of high-molar-mass NIPUs (M_n up to 95 kg × mol^{-1}) at a relatively low temperature (120°C). Additionally, stepwise temperature adjustments (135°C and 150°C) were carried out to enhance polymerization efficiency, yielding NIPUs with improved molar masses. This method promotes the synthesis of NIPUs in a short time (~6 h), using milder temperatures and three different diols. Further polymerization with different renewable diols led to NIPUs with tunable thermal properties, as assessed by differential scanning calorimetry (DSC) and thermogravimetric analysis (TGA), exhibiting relatively suitable thermal stability and semi-crystalline behavior associated with TPUs.

1 | Introduction

Polyurethanes (PUs) are versatile polymers offering a wide range of adjustable properties due to the variety of potential monomers, especially polyols, that are available for their synthesis. PUs are typically applied as foams, coatings, adhesives, or thermoplastic elastomers [1–3], and are commercially produced by the polyaddition reaction between diisocyanates and polyols [1–3]. However, the necessary diisocyanates are synthesized by the reaction of diamines and phosgene, which is a very hazardous and toxic chemical [4]. Furthermore, isocyanates are also toxic compounds, and their use was recently restricted by REACH regulations [5]. In this perspective, more sustainable routes to polyurethanes without using isocyanates have been investigated, known as non-isocyanate polyurethanes (NIPUs) [1–3].

Currently, two main routes are established for the synthesis of NIPUs: (i) the aminolysis of cyclic carbonates leading to polyhydroxyurethanes (PHUs) and (ii) the polycondensation of carbamates with diols by transurethanization, yielding

PUs [1–3, 6]. With respect to PHUs, due to the presence of hydroxyl groups (primary or secondary) in the repeating unit, the properties are not comparable with classical PUs produced from isocyanates. In contrast to PHUs, NIPUs synthesized by transurethanization have the same chemical structure as classical PUs and, consequently, similar properties to these unsustainable counterparts [1, 2].

The polycondensation of carbamates can be achieved by the transurethanization reaction of dicarbamate monomers in the presence of diols [7]. Several routes are described to obtain dicarbamates by reacting diamines with dimethyl carbonate, resulting in dimethyl carbamate [3], with ditertbutyl dicarbonate, leading to bistert-butyl carbamate [7], or by Lossen rearrangement of hydroxamic acids in the presence of dimethyl carbonate and methanol to produce dimethyl carbamate [8].

However, the transurethanization of bismethylcarbamate is still limited due to low reactivity and the occurrence of side reactions, yielding low molar mass polymers [3]. To improve the effectiveness of bismethylcarbamate transurethanization, the reaction is usually performed in the presence of a catalyst, at high temperature (ranging between 160°C and 200°C) and under reduced pressure [9, 10]. However, it was reported that under these conditions, urea can be generated together with allophanates or biurets [11]. Moreover, these conditions are not compatible with all sorts of diols and dicarbamates. In particular, low molar mass derivatives are inadequate due to their volatility. This is a serious drawback considering the synthesis of PU elastomers with phase-segregated microstructure [12–14], which are classically obtained by the reaction of a flexible macrodiol, the *soft segment*, with stiffer short chain co-reactants based on a diisocyanate and a chain extender, the *hard segment* (Figure 1A (isocyanate route)) [15]. Usually, the flexible macrodiols are based on polyether or polyester structures, while the chain extenders are short chain alkyl diols. The final structure and morphology of the PU elastomers are very dependent on a large number of factors, including the chemical structure of the precursors and the polymerization procedure. In particular, two different procedures are commonly used for their preparation: (i) the "one-shot" procedure, where all the reactants are mixed at the desired stoichiometric ratios in the beginning, yielding a fairly random distribution of the soft and hard segments in the macromolecular backbone, (ii) the second approach, the "prepolymer method", consists of two steps: first an excess of the diisocyanate is reacted with the soft segment oligomer to form the isocyanate terminated "prepolymer", followed by the "chain extension" step where the prepolymer is reacted with a short chain alkyl diol. The "prepolymer method" can help in increasing the degree of phase segregation. However, its success depends on the use of a correct stoichiometric amount of chain extender in the second step, which usually requires the titration of the isocyanate content in the prepolymer mixture.

Considering transurethanization polymerization, the use of short chain alkyl diols as chain extenders is often complicated due to their high volatility [17, 18]. Some dicarbamates have also been reported as too volatile for the process [19]. To circumvent this issue, NIPU elastomers are generally synthesized via transurethanization using a two-step approach, resembling the "prepolymer method" used in the isocyanate route, with additional constraints (Figure 1B) [13, 16, 18, 20]. The first step consists of reacting the dicarbamate with an excess of alkyl diol at high temperature (140°C–160°C) under a moderated nitrogen flow to avoid any volatilization. Once the carbamate is fully consumed, the excess of diol is distilled off, to yield the *hard* macrodiol. The latter is subsequently engaged in a polycondensation reaction with a *soft* macrodiol. This approach is more intricated than the isocyanate route and is further compromised by the long reaction times. Alternatively, Burel et al. explored an approach based on a single step consisting of reacting a dicarbamate with stoichiometric amounts of butanediol and polyethylene glycol (PEG) [21]. The reactions were conducted at temperatures between 140°C and 160°C in the presence of TBD as a catalyst, and under nitrogen flow (no vacuum). Using this approach, they were able to obtain semicrystalline PU with relatively low molar masses, M_n, ranging from 7.0 to 16.0 kg × mol^{-1}.

In this work, the melt transurethanization of dimethyl dodecane-1,12-diyldicarbamate (**3**) and PEG (**4**) was investigated in detail at a relatively low temperature, T = 120°C, compatible with the use of short-chain alkyl diols under continuous vacuum (~1 mbar) (Figure 1C). Different conditions in terms of catalysts, stirring processes, and alcohol to carbamate ratio ([OH]/[Carb.]) were investigated. Using mechanical stirring in the presence of potassium tert-butoxide (KO*t*Bu) as a catalyst, high molar masses, up to 94 kg × mol^{-1}, were achieved. The method was subsequently applied to the one-shot reaction of the same dicarbamate with equimolar amount of PEG and short alkyl diols. Again, high molar mass PUs were obtained (up to 74 kg × mol^{-1}), some of which exhibiting two T_g's as measured by DSC. This strategy thus opens new avenues for the facile synthesis of high molar mass semicrystalline NIPUs.

2 | Materials and Methods

2.1 | Materials

Potassium methoxide (KOMe, 95%), dihydroxytelechelic polyethylene glycol (PEG) (**4**, M_n = 2050 g × mol^{-1}) and 1,12-dodecanediol (**6**, 99%, 202.33 g × mol^{-1}) were purchased from Sigma-Aldrich. 1,12-diaminododecane (**1**, 98%, 200.36 g × mol^{-1}), potassium tert-butoxide (KO*t*Bu, 97%, 112.21 g × mol^{-1}) and 1,5,7-triazabicyclo[4.4.0]dec-5-ene (TBD, 98%, 139.20 g × mol^{-1}) were purchased from TCI. Dimethyl carbonate (**2**, 99%, 90.08 g × mol^{-1}), and potassium carbonate (K_2CO_3, 99%, 138.21 g × mol^{-1}) were purchased from Acros Organics. 1,5-Pentanediol (**5**, 96%, 104.15 g × mol^{-1}). Dimethyl formamide (DMF, 99.8%) was obtained from VWR, and deuterated dimethyl sulfoxide (DMSO-d_6, 99.5%) was obtained from Eurisotop. All the reactants were used without any further purification.

2.2 | Methods

2.2.1 | Synthesis

2.2.1.1 | Synthesis of Dimethyl Dodecane-1,12-Diyldicarbamate (3). 1,12-Dodecanediamine (**1**, 50 g, 1 equiv. mol) was added to a 100 mL Schlenk flask with an excess

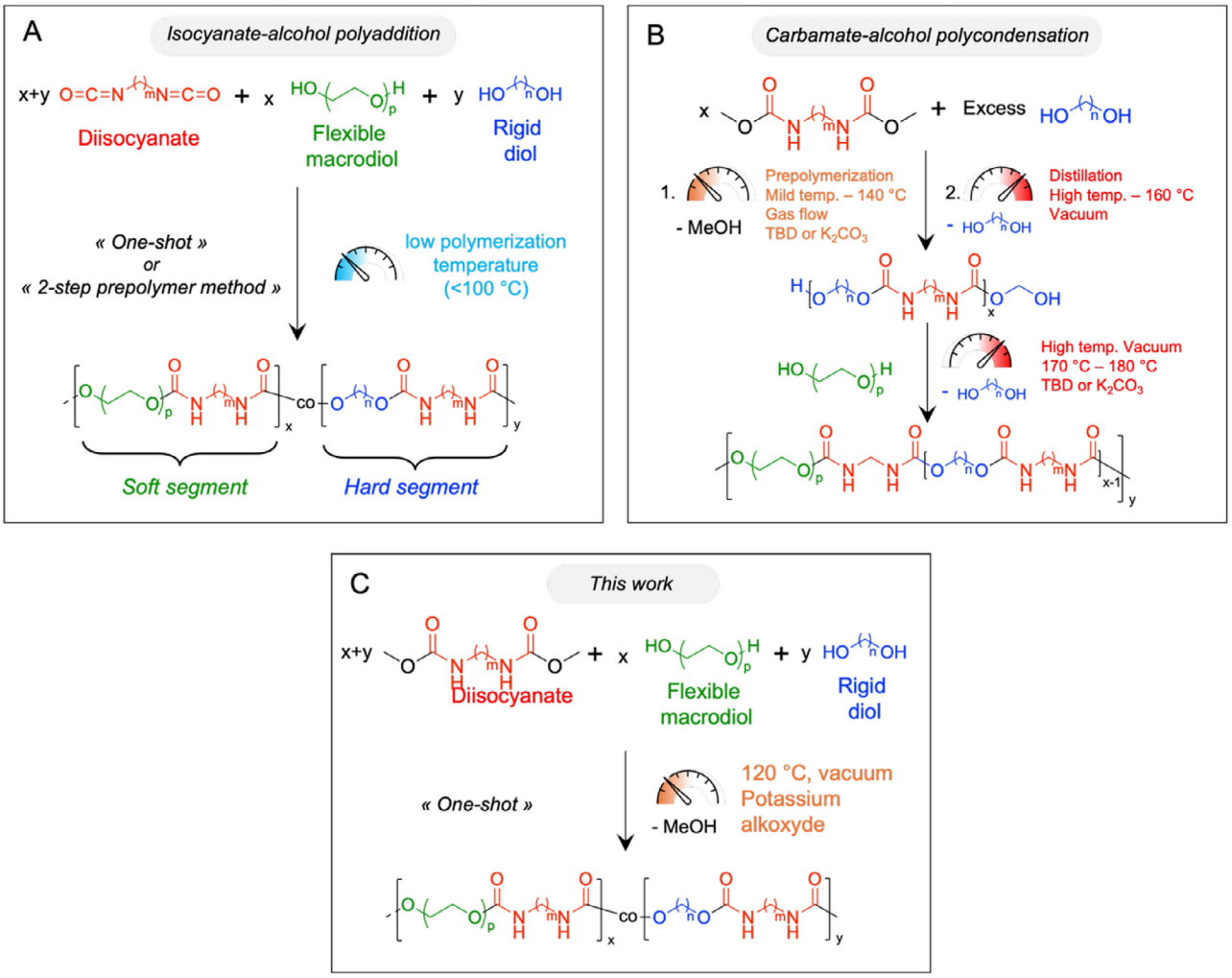

FIGURE 1 | Synthesis methods for PU elastomers with phase segregated microstructure. (A) Synthesis via the isocyanate-alcohol route [15]. (B) Synthesis via the carbamate–alcohol route as usually described in the literature [16]. (C) Method developed in this work.

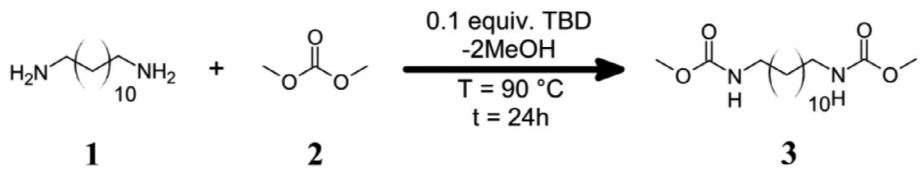

SCHEME 1 | Methoxycarbonylation of (**1**) in the presence of DMC (**2**) and TBD as a catalyst.

of dimethyl carbonate (**2**, 224.79 g, 10 eq. mol) in the presence of TBD as a catalyst (3.47 g, 0.1 eq. mol), as shown in the Scheme 1. The reaction was performed with magnetic stirring under an inert nitrogen atmosphere at 90°C for 24 h. Then, the excess of DMC and methanol generated during the methoxycarbonylation of the diamine was removed *in vacuo* at 65°C. Crude **3** was further purified by recrystallization from cold ice methanol. The product was filtrated and dried in a vacuum oven at 65°C for 12 h. Yield = 86%, T_m = 127°C. (^{1}H and ^{13}C NMR as well as FTIR spectra are available in ESI, Figures S1–S3)

2.2.1.2 | Transurethanization Optimization. Transurethanization of **3** with dihydroxy telechelic poly(ethylene glycol) (PEG, M_n = 2050 g × mol^{-1}) (**4**) was carried out in a 50 mL Schlenk-flask at 120°C (equipped with a magnetic (**NIPU 1b**) or an overhead mechanical stirring (**NIPU 1a**)). The monomers were mixed for 20 min under N_2 flush or until homogeneity, then different catalysts (0.1 equiv.) were added, such as potassium tert-butoxide (KO*t*Bu), potassium methoxide (KOMe, **NIPU 1c**), potassium carbonate (K_2CO_3, **NIPU 1d**), or 1,5,7-triazabicyclo[4.4.0]dec-5-ene (TBD, **NIPU 1e**), and then vacuum was applied (<1 mbar). Different alcohol:carbamate ratios ([OH]/[Carb.]) were assessed, varying from 0.8 to 1.05 equiv. mol (**NIPU 1a,f–j**, as displayed in Scheme 2). The transurethanization catalyst screening and monomer ratio were performed using overhead mechanical stirring for 12 h; the NIPUs coded as **NIPU 1a–j** were analyzed without any further purification.

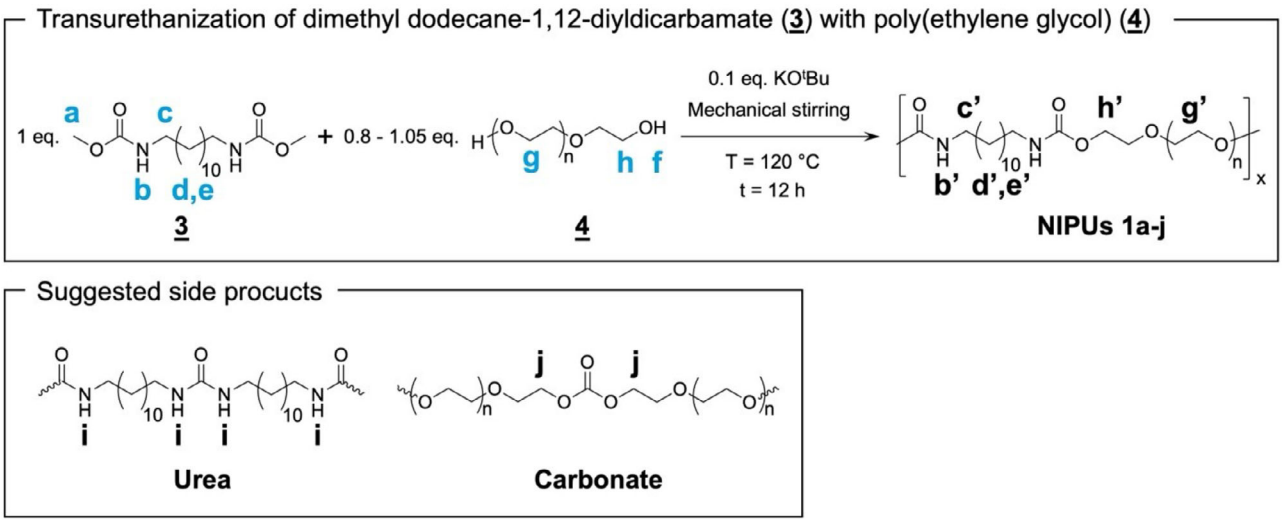

SCHEME 2 | Top: Synthesis of **NIPUs 1a–j** via the transurethanization of dodecane-1,12-diyldicarbamate **3** and dihydroxy telechelic poly(ethylene glycol) (PEG) **4**. Bottom: Representation of the suggested urea and carbonate side products.

2.2.1.3 | Synthesis of Polyurethanes With Short Chain Diols. Some polyurethanes were produced following the optimized conditions described in Section 3.1, i.e., the compounds were prepared using 0.1 equiv. of KO*t*Bu with respect to carbamate content applying a [OH]/[Carb.] molar ratio of 1:0.9. In this work, an equimolar amount of PEG and the short chain diol was used, i.e. 0.45 equiv. of PEG and 0.45 equiv. of the short chain diol, as compared to the dicarbamate. Two diols, both potentially biobased, were used, including 1,5-pentanediol (**5**, **NIPU 2**) and 1,12-dodecanediol (**6**, **NIPU 3a&b**). The reactants were added to a 50 mL round-bottom Schlenk flask and were homogenized at 120°C for ∼20 min under N_2 flow. Then the catalyst was added and the reaction mechanically stirred under vacuum for 12 h. In the case of the transurethanization of carbamate **3** with PEG and 1,12-dodecanediol (**5**), the reaction was also conducted using a higher temperature protocol according to the following temperature program: (i) 120°C for 6 h, (ii) 135°C for 4 h, and (iii) 150°C for 2 h, yielding NIPU 3b. The synthesized polymers were characterized without further purification.

2.2.2 | Characterization

^{1}H NMR was recorded on a Bruker Avance 400 spectrometer (400 MHz). The samples were solubilized in hot DMSO-d_6, and the analyses were performed at room temperature (∼25°C). From ^{1}H NMR, the alcohol and carbamate conversions were monitored in the course of the reaction by considering the signals of the OH protons of the alcohols and the NH protons of the carbamates, respectively, using a previously reported method [17]. Moreover, ^{1}H NMR was also used to estimate the urea and the carbonate contents in the final polymers. The detailed procedures are described in the Electronic Supplementary Information (ESI) (Figure 2).

Size exclusion chromatography (SEC) was used to estimate the polymer number-average molar mass (M_n), weight average molar mass (M_w), and dispersity ($Đ$). Due to varying solubility of the prepared polymers, the analysis was performed either with dimethylformamide (DMF) and lithium bromide (1 g × L^{-1}) as eluent or HFIP containing 0.10 wt.% potassium trifluoroacetate. For SEC measurements using DMF as eluent, the analyses were performed with an Ultimate 3000 system from Thermoscientific equipped with a diode array detector (DAD) and a differential refractive index detector (dRI) from Wyatt Technology. The polymers were separated using a set of two columns GF310+510 Asahipak containing polyvinyl alcohol as stationary phase (7.5 × 300 cm, exclusion limit: 300 000) and a controlled temperature of 50°C. The samples were analyzed using a calibration with polystyrene standards. SEC in HFIP was performed at 30°C with a TOSOH ECOSEC HLC-8320 SEC system, at a solvent flow of 0.40 mL min^{-1} and a sample concentration of 1 mg×mL^{-1}. The analysis was performed on a three-column system: PSS PFG Micro precolumn (3.0 × 0.46 cm, 10 000 Å), PSS PFG Micro (25.0 × 0.46 cm, 1000 Å), and PSS PFG Micro (25.0 × 0.46 cm, 100 Å). The system was calibrated with linear poly(ethylene glycol) standards.

The thermal stability of the NIPUs was investigated by thermogravimetry analysis (TGA). The analysis was performed on the TGA Q500 from TA Instruments. Samples of ∼6 mg were heated from 30°C to 700°C at a heating rate of 10°C min^{-1} under a nitrogen atmosphere.

The NIPU thermal transitions were identified by differential scanning calorimetry (DSC) using a DSC Q2000 from TA. The samples were weighed (∼6 mg) and analyzed using a standard aluminum crucible, three temperature ramps at a heating/cooling rate of 10°C min^{-1} were applied, the first from −100°C to 150°C, the second from 150°C to −100°C, and the last from −100°C to 200°C.

3 | Results and Discussion

3.1 | Transurethanization Optimization at 120°C

In this study, the transurethanization reaction of dimethyl dodecane-1,12-diyldicarbamate (**3**) with the dihydroxy telechelic

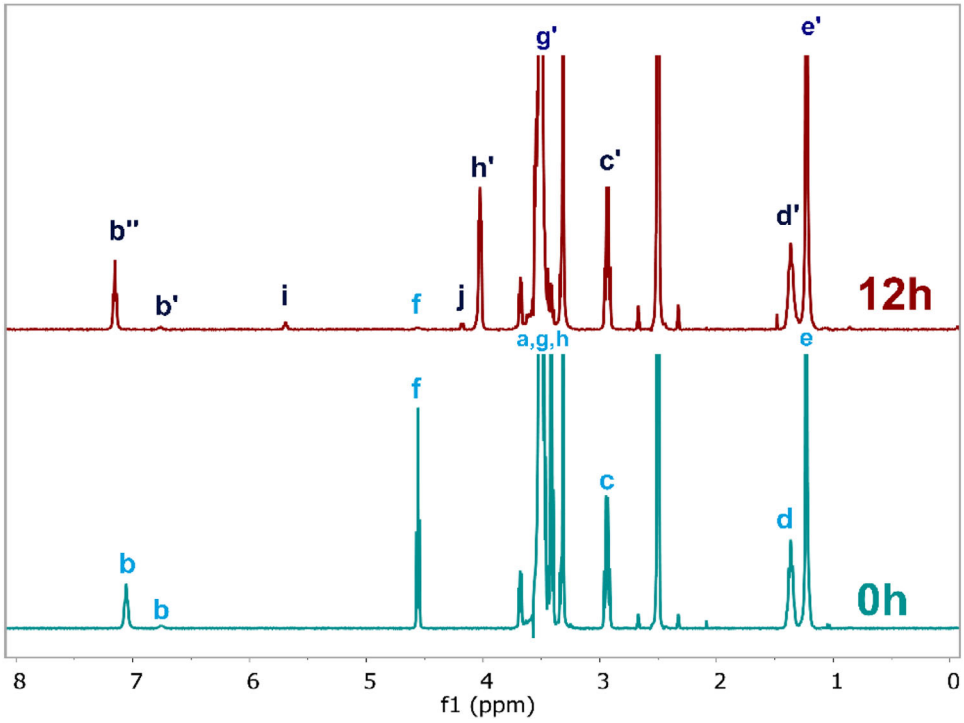

FIGURE 2 | ^{1}H NMR monitoring for the transurethanization of dodecane-1,12-diyldicarbamate **3** and dihydroxy telechelic poly(ethylene glycol) (PEG) **4**, during the synthesis of **NIPU 1a** (bulk, [OH]/[Carb.] = 1.0, 0.1 equiv. KO*t*Bu, mechanical stirring, T = 120°C). Aliquots were collected from the crude product and analyzed in DMSO-d_6.

poly(ethylene glycol) (PEG) (**4**) was conducted at 120°C under various conditions (Scheme 2). In all cases, the reaction was followed by ^{1}H NMR, in DMSO-d_6, in order to monitor the hydroxyl and the carbamate conversions. Figure 2 shows the ^{1}H NMR spectra for the reaction performed in the presence of potassium tert-butoxide (KO*t*Bu) as a catalyst, with a hydroxyl to carbamate ratio [OH]/[Carb.] = 1.00, using overhead mechanical stirring (150 rpm), for t = 0 and t = 12 h (**NIPU 1a**, Table 1, entry 1). The signal related to the NH protons of the bismethylcarbamate (**b**, 7.06 ppm) and the one associated with the OH protons of the diol (**f**, 4.56 ppm) continuously decrease over time, while the polyurethane carbamate NH proton signal (**b'**, 7.15 ppm) increases. These signals were used to calculate the conversions. The plots of the conversions as a function of time are available in the ESI, Figure S4. For **NIPU 1a**, the carbamate conversion was 98.2% after 12 h, while the OH conversion was 90.9%. The transurethanization reaction was further investigated by ^{13}C NMR, as illustrated in Figure S5. A characteristic peak at 156 ppm confirms the presence of the carbamate carbonyl, while signals at 64 and 78 ppm were assigned to the α- and β-methylene carbons of the reacted PEG segment, respectively [22]. The presence of these signals supports the successful polymerization by transurethanization. In addition, the signal of the methyl carbon from the starting carbamate at 53 ppm is not present, indicating the complete conversion of this terminal group [22]. However, residual signals at 62 and 73 ppm, corresponding to the α- and β-methylene carbons of unreacted PEG, are still observed. This suggests a partial consumption of the diol and indicates a difference in conversion between the dicarbamate and diol monomers under the applied reaction conditions [22].

As discussed elsewhere [11, 20], and notably in our previous work [17], the discrepancy between the two values is related to the occurrence of side reactions, notably carbamate cross-metathesis, which generates dimethyl carbonate and urea. The mechanisms associated with these side reactions are displayed in Scheme S1. Supporting their occurrence, amino protons associated with urea (**i**, 5.69 ppm) and carbonate (**j**, 4.08 ppm) linkages were identified (Figure 2). After 12 h, the relative urea and carbonate contents of **NIPU 1a** were around 5.1 and 1.9 mol%, respectively, as calculated based on the total molar ratio of the carbamates, urea, and carbonate protons (see ESI, Equations S1 and S2). The side products were further confirmed by COSY through the correlation between signal **i** (assigned to NH protons) and signal **c** (associated with the α-methylene protons of carbamate or urea groups), as shown in Figure S6 [22]. This correlation supports the presence of urea-containing species. Additionally, signals consistent with carbonate formation were also observed by HMBC NMR (Figure S7), through the correlation of the carbonate's carbonyl carbon (~63 ppm) with α-proton from reacted PEG. This further indicates the occurrence of side reactions during the transurethanization process [22].

The conversions and the side product contents were similar to those reported for transurethanization polymerizations in the literature, despite the unusually low temperature used in this first test. To our knowledge, such reactions are typically performed at temperatures ≥160°C [16, 18, 20, 23], with only a handful of examples reporting conditions at 140°C [21]. The results obtained for **NIPU 1a** demonstrate that the reaction can be performed at 120°C. This is further confirmed by considering the high molar mass obtained for **NIPU 1a** (SEC DMF: M_n

TABLE 1 | Characteristics of the NIPUs obtained via transurethanization reaction of **3** with PEG and diol chain extenders.

Entry	NIPU	Catalyst	$\frac{[OH]}{[Carb.]}$	M_n[a] [kg × mol^{-1}]	M_w[a] [kg × mol^{-1}]	$M_{n,NMR}$[b] [kg × mol^{-1}]	$Đ$[a]	OH conversion[c] [%]	Carbamate conversion[c] [%]	Urea content[c] [%]	Carbonate content[c] [%]
1	**1a**	KO*t*Bu	1.00	36.4	77.9	25.3	2.2	90.9	98.2	5.1	1.8
2	**1b**[d]	KO*t*Bu	1.00	12.0	16.5	8.3	1.4	72.3	75.8	2.2	0.02
3	**1c**	KOMe	1.00	37.5	79.0	26.5	2.1	91.3	96.9	4.9	2.5
4	**1d**	K_2CO_3	1.00	21.3	37.2	28.1	1.8	91.8	94.6	1.2	1.5
5	**1**[e]	TBD	1.00	7.4	8.2	4.0	1.1	42.9	49.9	0.0	0.0
6	**1f**	KO*t*Bu	1.05	27.1	73.4	25.9	2.7	91.1	97.7	4.7	2.5
7	**1g**	KO*t*Bu	0.98	42.3	88.4	27.6	2.1	92.6	98.8	4.5	2.1
8	**1h**	KO*t*Bu	0.95	47.7	113.6	29.8	2.3	94.7	98.6	5.5	2.3
9	**1i**	KO*t*Bu	0.90	61.7/26.0[g]	192.7/139.3[g]	23.4	3.1/5.4[g]	95.2	98.9	4.9	3.03
10	**1j**	KO*t*Bu	0.80	33.2[f]	151.7[f]	n.a.[f]	4.7[f]	n.a.[f]	n.a.[f]	n.a.[f]	n.a.[f]
11	**2**	KO*t*Bu	0.90	19.4[g]	46.3[g]	20.8	2.4[g]	98.6	99.5	5.1	0.7
12	**3a**	KO*t*Bu	0.90	6.3[g]	7.32[g]	4.2	1.2[g]	71.1	68.7	1.4	0.8
13	**3b**	KO*t*Bu	0.90	14.7[g]	27.1	21.5	1.8	98.8	90.5	1.4	0.6

[a]Obtained by SEC analysis in DMF using polystyrene standards;
[b]Mn calculated based on ^{1}H NMR, the Equation S3;
[c]Estimated by ^{1}H NMR;
[d]Prepared with magnetic stirring;
[e]Prepared with mechanical stirring;
[f]Sample was only partially soluble;
[g]Obtained by SEC analysis in HFIP using PEG standards.

= 36.4 kg × mol^{-1}, $Đ$ = 2.15, Figure S8 and Table S1). These values are comparable to [23], or higher [18, 21] than those reported in the literature for transurethanization polymerizations performed at higher temperatures. M_n was also estimated using the conversion of the OH groups as measured by ^{1}H NMR. Based on the Carother's equation (see ESI, Equation S3), we found $M_{n,NMR}$ = 28.1 kg × mol^{-1} in close agreement with the value measured by SEC.

A critical parameter for the success of the reaction at 120°C is mechanical stirring. This is well illustrated by comparing the evolution of M_n during the polymerization catalyzed by KO*t*Bu, performed with either magnetic (**NIPU 1b**) or overhead mechanical stirring (150 pm) (**NIPU 1a**), as shown in Figure 3 (SEC elugrams are available in the ESI, Figures S8 and S9). After 1 h of reaction, both mixing methods show similar M_n of ~10 kg × mol^{-1} (SEC, DMF). However, beyond 1 h, this value remained rather constant for magnetic stirring, whereas the mechanically stirred reaction showed a significant further increase of M_n to almost 40 kg × mol^{-1} (SEC, DMF). This result confirms that the progress of the transurethanization depends on effective mixing, which is not achieved using magnetic stirring due to the viscosity increase at the relatively low temperature of 120°C in the course of the polymerization [24]. The **NIPU 1a** prepared using mechanical stirring achieved a maximum value of 39.5 kg × mol^{-1} (SEC, DMF) and a dispersity, $Đ$, of 2.05 after 8 h, reaching a conversion of OH and methyl carbamates of 90.9% and 98.2%, respectively. In contrast to reaction times reported in the literature for this kind of polymerization, e.g. >15 h, this result indicates a faster and more practicable approach. In fact, after 12 h, a substantial decrease in M_n to 36 kg × mol^{-1} was observed, indicating that longer reaction times can be detrimental due to the promotion of undesired side reactions [7].

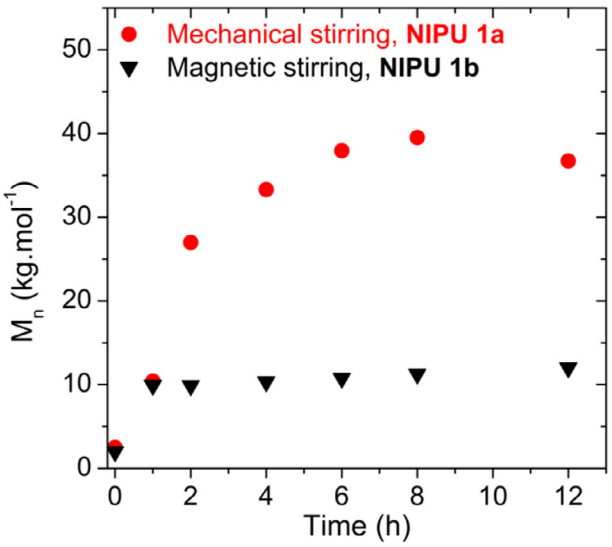

FIGURE 3 | Comparison of molar mass obtained by SEC in DMF at different reaction times for the synthesis of **NIPU 1** via (i) overhead mechanical stirring (150 rpm) (**1a**) and (ii) magnetic stirring (**1b**) (bulk, [OH]/[Carb.] = 1.0, 0.1 equiv. KO*t*Bu, T = 120°C).

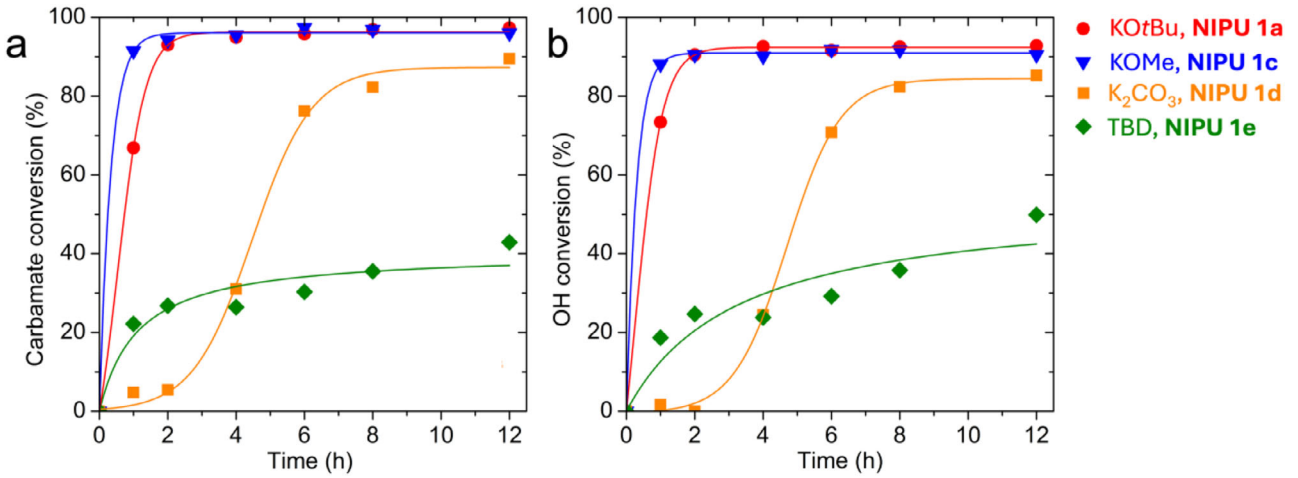

FIGURE 4 | ^{1}H NMR monitoring of (a) carbamate conversion and (b) OH conversion in the course of **NIPU 1** synthesis prepared at 120°C with different catalysts: KO*t*Bu (**1a**), KOMe (**1c**), K_2CO_3 (**1d**), and TBD (**1e**) (bulk, [OH]/[Carb.] = 1.0, mechanical stirring). The crude product was solubilized in DMSO-d_6.

The effectiveness of the mechanical stirring is also corroborated by the difference in the functional group conversion. Indeed, mechanical stirring results in a conversion of 90.9% and 98.2% of carbamate and OH functional groups, respectively, while in the case of magnetic stirring (**NIPU 1b**), the conversion was less than 76% for both carbamate and OH reactive functions.

Another key factor in ensuring the efficient progress of the reaction at 120°C is the choice of catalyst. To date, the catalysts that were the most commonly used for transurethanization polymerization are K_2CO_3 [16, 20, 23] and TBD [21]. However, K_2CO_3 can suffer from low solubility issues at moderate temperatures, while TBD is often considered as unstable in the typical temperature range of transurethanization reaction. In this work, KO^{t}Bu was chosen for its promising balance in terms of solubility, stability, and basicity. To our knowledge, only one prior study reported its use for the polymerization of di-BOC isophorone diamine with different polyether diols and diamines [7]. Herein, its superior efficiency for the transurethanization reaction of dimethylcarbamate with diols at 120°C was illustrated by comparison with KOMe, K_2CO_3, and TBD. Figure 4 represents the carbamate and OH conversions monitored by ^{1}H NMR for the preparation of **NIPU 1** (T = 120°C, overhead mechanical stirring 150 rpm, <1 mbar, 12 h) catalyzed by 0.1 equiv. of KO*t*Bu (**NIPU 1a**), KOMe (**NIPU 1c**), K_2CO_3 (**NIPU 1d**), and TBD (**NIPU1e**). The catalysts were added after monomers mixing (at 120°C for ~20 min under N_2 flow). The polymerization reactions were also monitored using SEC chromatography, and the associated data are available in the ESI (Figures S8 and S10–S12 as well as Tables S1 and S3–S5).

As expected, TBD showed the worst transurethanization performance of the series after 12 h of reaction, with a maximum conversion of 42.9% and 49.9% for OH and carbamate functions, respectively, yielding **NIPU1e** with M_n = 7.4 kg × mol^{-1} (SEC, DMF, Table 1, Entry 5). Similar molar masses (M_n <10 kg × mol^{-1}) were reported by Burel et al. for the transurethanization polymerization of various alkyl dimethyl carbamates with PEG (1500 g × mol^{-1}) and butanediol, catalyzed by TBD at temperatures varying from 140°C to 160°C. In fact, the lower catalytic efficiency of TBD for carbamate transurethanization is now well established and attributed to different factors, including the thermal instability of TBD in the temperature range required for transurethanization reaction [3], the lack of TBD base strength to deprotonate the nitrogen group of the carbamate [7], and the thermodynamic penalty due to the coordination of carbamate group with both nitrogen groups from TBD [25].

The results obtained with K_2CO_3 (**NIPU 1d**) confirm the solubility issues associated with this catalyst. Indeed, the plot of the conversion as a function of time exhibits a sigmoidal shape, suggesting a delayed action of the catalyst. This latency is likely due to the gradual reaction of K_2CO_3 with methanol, produced during the initial stage of the transurethanization reaction. This well-documented reaction yields potassium methoxide (KOMe) and potassium bicarbonate ($KHCO_3$) [26], with KOMe being the actually active catalyst to its higher solubility and basicity (pKa(KOMe) = 15.5 vs. pKa(K_2CO_3) = 10.25). The progressive liberation of KOMe is expected to enable the delayed catalysis of the polymerization reaction, as evidenced by the conversion plots. In the end, after 12 h of reaction, the OH conversion reaches a maximum value of 85.3%, while a M_n = 21.3 kg × mol^{-1} was observed (SEC, DMF, Table 1, entry 4). These results are inferior to those achieved with KO*t*Bu, further confirming that K_2CO_3 is less suitable than KO*t*Bu for polymerization at 120°C.

Finally, KOMe was directly tested as a catalyst (**NIPU 1c**). As expected, it exhibits excellent performance comparable to KO*t*Bu (Table 1, entry 3). These results highlight that potassium alkoxides are well suite catalysts for the transurethanization reactions performed at moderated temperature, i.e. 120°C. Their better catalytic activity is well explained by their higher basicity, as well as better miscibility. Regarding the side reactions, both catalysts exhibited a similar amount of urea (~5 mol%), while KOMe showed a slightly higher carbonate content (2.5 mol%) than KO*t*Bu (1.9 mol%). Thus, KO*t*Bu was used in the rest of the study.

Overall, these results demonstrate that the combination of efficient stirring with a well-miscible base catalyst enables the

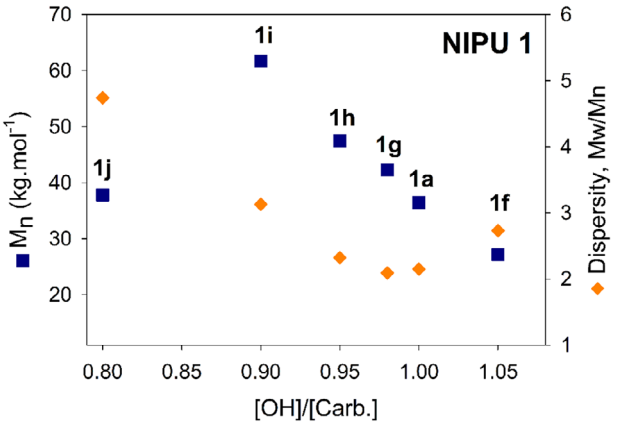

FIGURE 5 | Influence of the stoichiometric ratio [OH]/[Carb.] on the molecular weight and dispersity (both obtained by SEC in DMF) in the synthesis of **NIPU 1a, f–j**, after 12 h of reaction time (bulk, mechanical stirring, 0.1 equiv. KO*t*Bu, T = 120°C).

efficient transurethanization reaction at relatively low temperature. These conditions are particularly well-suited for the use of short alkyl diols. Before pursuing in this direction, the reaction was further optimized in terms of alcohol to carbamate ratio ([OH]/[Carb.]). Indeed, as discussed above, carbamate metathesis side reactions during transurethanization generate urea moieties and cause a carbamate and OH conversion discrepancy [11, 27, 28]. This divergence in the A-A and B-B monomer conversion leads to a stoichiometry penalty, which results in a reduction of the molar mass and in branching or, ultimately, cross-linking [16, 29]. In this context, [OH]/[Carb.] was varied between 0.80 and 1.05, and its impact on the molar mass of **NIPUs 1a** and **1f–j** (Table 1, entries 1 and 6–10) was investigated by SEC (elugrams available in the ESI, Figures S13–S17 and Tables S6–S10, Plot of M_n as a function of time in Figure S18). The evolution of M_n as a function of [OH]/[Carb.] is shown in Figure 5. Clearly, M_n exhibits a maximum for [OH]/[Carb.] = 0.9 (**NIPU 1i**, entry 9), with M_n = 61.7 kg × mol^{-1} and M_w = 192.7 kg × mol^{-1} ($Đ$ = 3.06), recorded by SEC in DMF. This is further illustrated by the highest alcohol (95.2%) and carbamate (98.9%) conversions achieved at this ratio [16, 30, 32,]. Conveniently, the molar mass of **NIPU 1i** is comparable to those of classical TPUs prepared with diisocyanates and polyols as reported in the literature [20, 31, 32]. Importantly, at [OH]/[Carb.] = 0.8 (**NIPU 1j**), the NIPU obtained is partially insoluble in DMF and insoluble in DMSO-d_6. This is most certainly due to the formation of cross-linking points via the generation of allophanates and biurets in the presence of a high excess of carbamates [7, 16]. Interestingly, the molar mass estimated from the OH conversion measured by NMR, $M_{n,\,NMR}$ (Table 1), follows a similar trend to that obtained from SEC. However, the maximum value occurs at a [OH]/[Carb.] ratio of 0.95. This deviation is likely due to the dependence of $M_{n,\,NMR}$ on the [OH]/[Carb.] ratio as described by the Carother's equation (see ESI for detailed calculation, Equation S3). Since the SEC measurement provides a more direct assessment of M_n , the ratio [OH]/[Carb.] = 0.9 is considered the optimal condition for maximizing molar mass.

In summary, the transurethanization of dimethyl dodecane-1,12-diyldicarbamate (**3**) with the dihydroxy telechelic poly(ethylene glycol) (PEG) (**4**) was successfully optimized at a relatively low temperature, 120°C, using KO*t*Bu as a highly stable and soluble catalyst, with an alcohol-to-carbamate ratio of [OH]/[Carb.] = 0.9. High molar masses (M_n >60 kg × mol^{-1}) can be obtained in less than 8 h of reaction under vacuum. This new system is more efficient than conventional examples previously reported in the literature for the polymerization of similar dicarbamates and PEG. For instance, Burel et al. reported a maximum molar mass of 10 kg × mol^{-1} after 16 h under argon flow using TBD at 140–160°C [21]. Notably, this new methodology expands the potential of transurethanization to mixtures of diols, including short alkyl diols, which are typically volatile under conventional reaction conditions, as will be explained below.

3.2 | Transurethanization With Mixtures of Diols at 120°C

To demonstrate the potential of the new transurethanization conditions developed in this study, a series of NIPUs were synthesized by reacting dicarbamate **3** with equimolar content of dihydroxy telechelic PEG (**4**) and short chain alkyl diols. Two alkyl diols were used: (i) 1,5-pentanediol (**5**) yielding polymer referenced as **NIPU 2**, and (ii) 1,12-dodecanediol (**6**) yielding polymer referenced as **NIPU 3**. They will be compared to **NIPU 1** obtained using PEG (**4**) as the only diol. The monomers ratio used for the synthesis of each NIPU is summarized in Table 2. It is worth mentioning that both alkyl diols (**5** & **6**) can be potentially biobased. The 1:1 ratio of flexible (PEG) and rigid (alkyl) diols is typical when targeting semicrystalline TPU [12, 13, 21]. The transurethanization was performed following the optimized protocol, i.e., mechanical stirring, 120°C, [OH]/[Carb.] = 0.90 with KO*t*Bu as catalyst (Scheme 3). The catalyst was added when the reaction medium achieved homogeneity.

The efficiency of the transurethanization reactions was assessed by monitoring the OH and carbamate conversions via ^{1}H NMR, and by following the molar mass development by SEC. Due to the insolubility of the resulting polymers in DMF, their molar masses were assessed through SEC using hexafluoroisopropanol (HFIP) as solvent (PEG calibration). The results are collected in Table 1, entries 11–13.

In the case of **NIPU 2** (Table 1, entry 11) prepared by the transurethanization of dimethyl dodecane-1,12-diyldicarbamate (**3**) with poly(ethylene glycol) (**4**) and pentanediol (**5**), both the OH and the carbamate conversions reached high values, 98.6% and 99.5% respectively, comparable to the synthesis of **NIPU 1** (Detailed NMR characterization available in the ESI, Figures S19–S22). This illustrates the suitability of the method for the use of a short chain alkyl diol in combination with a macrodiol. It is further confirmed by considering the molar mass of **NIPU 2** (SEC HFIP, M_n = 19.4 kg × mol^{-1}, $Đ$ = 2.4). The corresponding chromatogram is presented in Figure 6. Importantly, the relative contents of urea and carbonate moieties, 5.2 and 0.7 mol% respectively, are also comparable to those found for **NIPU 1**. As a comparison with the literature, when using a short alkyl diol such as 1,5-pentanediol in a more conventional protocol (magnetic stirring, vacuum, 150°C–180°C, K_2CO_3), very high contents in urea were observed (>25 mol%) [17]. This was attributed to the stoichiometric imbalance resulting from the partial evaporation of the alkyl diol in these conditions.

TABLE 2 | Reactant ratio used for the synthesis of NIPUs 1–3.

Entry	NIPU	Dicarbamate (3)	PEG (4)	1,5-Pentanediol (5)	1,12-dodecanediol (6)
1	**NIPU 1 (i)**	1 eq.	0.9 eq.	—	—
2	**NIPU 2**	1 eq.	0.45 eq.	0.45 eq.	—
3	**NIPU 3 (a&b)**	1 eq.	0.45 eq.	—	0.45 eq.

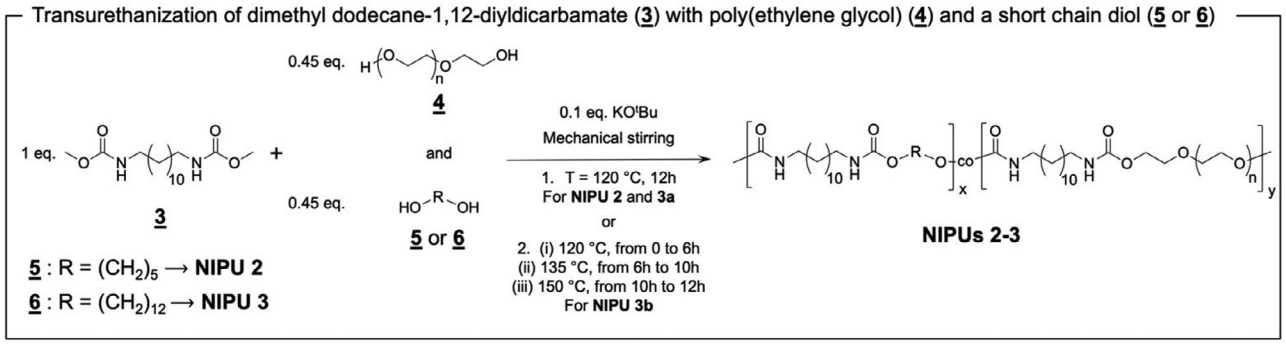

SCHEME 3 | Synthesis of **NIPUs 2** and **3** via the transurethanization of bismethylcarbamate **3** with renewable diols **5** or **6** and the molecular structures of **2–5**, in combination with PEG-diOH **1**.

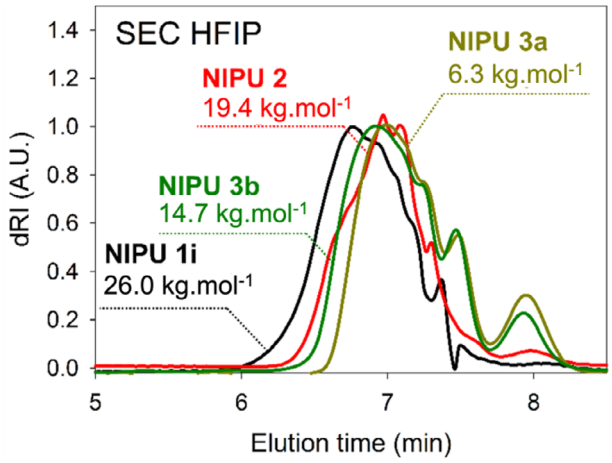

FIGURE 6 | SEC chromatograms in hexafluoroisopropanol (HFIP) of the **NIPUs 1–3** obtained by transurethanization of **3** with **4** (**NIPU 1i**), and 1,5-pentanediol (**5**) (**NIPU 2**) and 1,12-dodecanediol (**6**) (**NIPU 3a** and **3b**) at a temperature of 120°C using 0.1 equiv. mol of KO*t*Bu and a [OH]/[Carb.] of 0.9:1.0.

NIPU 3 was first prepared using the optimized protocol, i.e. 12 h of reaction at 120°C and vacuum of <1 mbar. The characteristics of the resulting polymer, labelled as **NIPU 3a**, are collected in Table 1, entry 12. They reveal that the polymerization did not proceed well. Indeed, both the OH and the carbamate conversions plateau around 70% (NMR spectra available in the ESI, Figure S23). Furthermore, the molar mass of the resulting polymer (SEC HFIP, $M_n = 6.3\,kg \times mol^{-1}$, $Đ = 1.2$) is very low compared to that of **NIPUs 1** and **2** (chromatogram available in Figure 6). However, the urea and carbonate content remained relatively low, thus suggesting that the poorer performances of this system are not related to a stoichiometric imbalance. Instead, it is the significant increase in the viscosity that seems to be responsible for hindering proper mixing [33]. As previously discussed, effective mixing is crucial for producing high-molar-mass polymers [24].

In this case, the high viscosity of the polymer arises from conducting the transurethanization at temperatures below its melting point, which will be discussed below. To illustrate this point, **NIPU 3** was synthesized using a three-step temperature protocol, as follows: (i) 120°C for 6 h, (ii) 135°C for 4 h, and (iii) 150°C for 2 h. The resulting polymer, designated as **NIPU 3b**, is listed in Table 1, entry 13. Under these conditions, the conversion reached 98.8% for hydroxyl (OH) and 90.5% for methyl carbamate groups, comparable to those observed for **NIPUs 1** and **2** (NMR spectra available in the ESI, Figure S24). The success of the three-step temperature protocol is further evidenced by the higher molar mass of **NIPU 3b** (SEC HFIP, $M_n = 14.7\,kg{\cdot}mol^{-1}$), as shown in the chromatogram in Figure 6. Despite the higher temperatures used in this program, the overall conditions remain milder than conventional methods reported in the literature (≥160°C). Notably, the initial step at 120°C, in the presence of KO*t*Bu, facilitates rapid oligomerization, which is crucial for preventing volatilization and maintaining stoichiometric balance.

These results highlight the potential of the conditions developed in this study for designing new temperature protocols compatible with various diol mixtures, including volatile diols. Additionally, the viscosity behavior of **NIPU 3b** suggests that these polymers may exhibit high melting temperatures, which is of practical interest in the field of TPU materials. This aspect is further explored in the next section through an analysis of their thermo-mechanical properties.

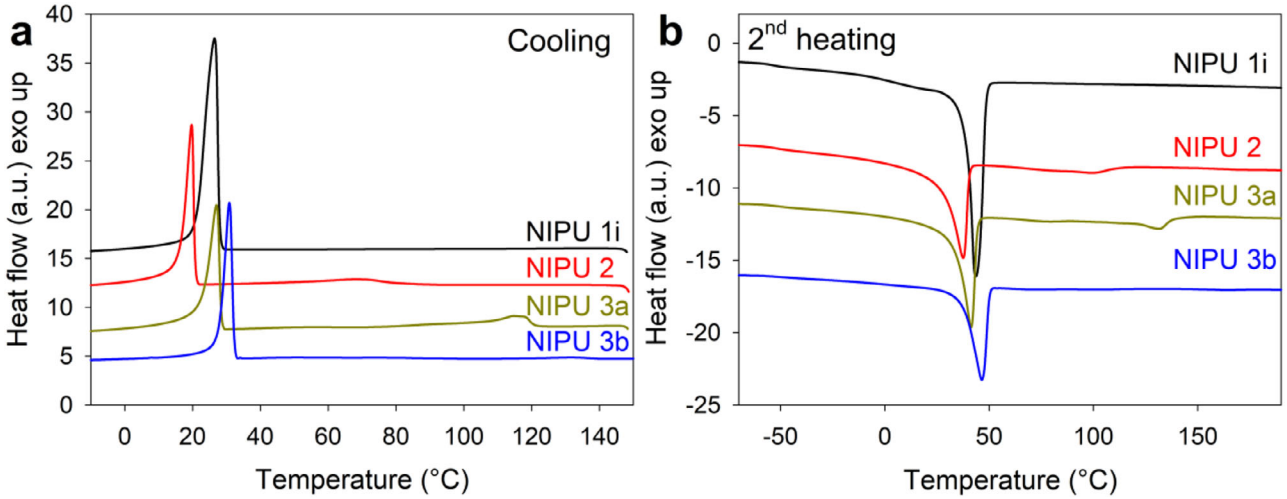

FIGURE 7 | DSC Curves of the partially biobased **NIPUs 1 to 3** ((1) 10°C/min (a) cooling ramp, (b) 2nd heating ramp).

TABLE 3 | Thermal properties of NIPUs 1–3 obtained by DSC and TGA.

	Soft domains					*Hard domains*					
	T_{g1}[a] [°C]	T_{m1}[a] [°C]	ΔH_{m1}[b] [J g^{-1}]	T_{c1}[a] [°C]	ΔH_{c1}[b] [J g^{-1}]	T_{g2}[a] [°C]	T_{m2}[a] [°C]	ΔH_{m2}[b] [J g^{-1}]	T_{c2}[a] [°C]	ΔH_{c2}[b] [J g^{-1}]	*$Td_{5\%}$*
NIPU 1i	−54	44	108.9	26	90.7	—	—	—	—	—	299
NIPU 2	−52	37	65.6	19	56.3	62	100	7.2	69	12.5	280
NIPU 3a	−51	41	63.8	27	58.3	71	132	9.5	115	16.1	271
NIPU 3b	−49	46	68.5	31	59.0	112	163	0.9	131	2.1	—
PEG	—	56	156.9	33	148.7	—	—	—	—	—	—

[a]T_g, T_m, and T_c are the glass transition, melting, and crystallization temperatures;
[b]ΔH_m and ΔH_c are melting enthalpy and crystallization enthalpy, respectively. T_g was measured from the second heating cycle of the DSC analyses.

3.3 | Thermal and Mechanical Properties of NIPUs Obtained by Transurethanization at 120°C

NIPUs 1, 2, and 3 (Table 2) were characterized by DSC, TGA, FTIR, and tensile tests. For comparison purposes, we compared the NIPUs obtained using the optimized transurethanization protocol i.e., mechanical stirring, 120°C, [OH]/[Carb.] = 0.90 with KO*t*Bu as catalyst: **NIPU 1i**, **NIPU 2,** and **NIPU 3a**. **NIPU 3b** synthesized using a three-step temperature protocol ((i) 120°C for 6 h, (ii) 135°C for 4 h, and (iii) 150°C for 2 h) was also included in this study. The DSC traces recorded from the cooling and the second heating cycles are shown in Figure 7. The characteristics of the corresponding thermal transitions are collected in Table 3.

NIPU 1i clearly exhibits the behavior of a semi-crystalline polymer with one exothermic peak characteristic of crystallization on the cooling cycle (T_c = 26°C) and an endothermic peak typical of a melting point on the heating cycle (T_m = 44°C). Additionally, a glass transition is clearly visible on the heating cycle (T_g = −54°C). These values are lower than those of the starting PEG diol (Table 3). The same transitions are visible for the thermogram of **NIPU 2** (T_{g1} = −52°C, T_{m1} = 37°C, and T_{c1} = 19°C) along with broader melting and crystallization peaks at higher temperatures, observed at T_{m2} = 100°C and T_{c2} = 69°C, respectively. Similarly, an additional glass transition is visible at T_{g2} = 62°C, in the heating cycle. The thermograms recorded from **NIPU 2** suggest partial phase separation, with PEG-rich soft domains (T_{g1}, T_{m1}, and T_{c1}) and hard domains rich in rigid units (pentane alkyl chains, from **5**) and urethane moieties (T_{g2}, T_{m2}, and T_{c2}). Similar thermal behavior was reported for isocyanate-based polyurethane derived from the reaction of PEG diols with 1,6-hexamethylene diisocyanate and 1,4-butanediol as a chain extender [34]. These results suggest that the methodology developed in this study could be suitable for the one-shot synthesis of PU exhibiting some degree of microphase separation.

The possibility to observe two microphases with our synthesis strategy is further confirmed by considering the results obtained for **NIPUs 3a** and **3b**. The thermal properties of the softer microphase (T_{g1} = −51°C, T_{m1} = 41°C, and T_{c1} = 27°C) closely resemble those of **NIPU 2**, as expected, given that the behavior of this phase should be primarily governed by the thermal properties of the PEG diol. In contrast, the harder microphase (T_{g2} = 71°C, T_{m2} = 132°C, and T_{c2} = 115°C) exhibits significantly higher temperatures than that of **NIPU 2**. This suggests a higher degree of crystallinity within the hard domains when 1,12-dodecanediol

(**6**) is used as a rigid diol [34]. Importantly, T_{m2} is above 120°C, which explains why the reaction does not proceed well using a single polymerization temperature of 120°C. Additional steps at T = 135°C (~T_{m2}) and T = 150°C (>T_{m2}) were necessary to complete the reaction. **NIPU 3b** exhibits hard domains with further increased transition temperatures (T_{g2} = 112°C, T_{m2} = 163°C, and T_{c2} = 131°C); however, the associated enthalpies are much smaller. In fact, those transitions are barely visible on the thermograms represented in Figure 6. Only by magnifying the region comprised between 50°C and 180°C, the melting and crystallization peaks (Figure S25) can be observed. This suggests that the progress of the one-shot polymerization is detrimental to phase segregation, due to a uniform distribution of the rigid and flexible diols along the polymer chains at higher degrees of polymerization. Further optimization of the reaction, notably in terms of soft-to-rigid alcohol ratio, or a "soft segment" first pre-polymerization, could help in restoring a better segregation.

To further support the occurrence of partial phase segregation in NIPUs derived from mixtures of flexible and rigid diols, a detailed analysis of their FTIR spectra was performed. The carbonyl (C═O) stretching vibrations in urethane linkages are highly sensitive to hydrogen bonding and molecular ordering, making FTIR spectroscopy a powerful tool for assessing microstructural organization. Specifically, FTIR enables the quantification of urethane groups engaged in ordered hydrogen bonding, which serves as an indirect indicator of microphase separation [20, 35].

Figure 8a presents the full FTIR spectra for **NIPUs 1i**, **2**, and **3a**. In all cases, the spectral features are consistent with polyurethane formation, as evidenced by: (i) the N–H stretching vibration around 3300 cm^{-1}, (ii) the N–H bending vibration near ~1530 cm^{-1}, and (iii) the C═O stretching region spanning 1600–1740 cm^{-1}, characteristic of urethane carbonyls [20, 21]. Within this latter region, multiple overlapping bands are observed due to varying hydrogen bonding environments and the presence of carbonyl-containing side products, including urea and carbonate species.

To resolve these contributions, spectral deconvolution was carried out (see Figure 8c,d and detailed methodology in the ESI) [17, 35]. Based on literature reports for NIPUs synthesized via transurethanization polymerization [17, 35], seven distinct carbonyl absorptions were identified: carbonate (~1740 cm^{-1}), free urethane (~1724 cm^{-1}), disordered hydrogen-bonded urethane (~1699 cm^{-1}), ordered hydrogen-bonded urethane (~1682 cm^{-1}), free urea (~1670 cm^{-1}), disordered hydrogen-bonded urea (~1660 cm^{-1}), and ordered hydrogen-bonded urea (~1630 cm^{-1}).

"Free" urethane and urea groups, unassociated with hydrogen bonds, are typically found in PEG-rich, amorphous domains, where spatial dilution hinders ordered hydrogen bonding. Disordered hydrogen-bonded species correspond to short-range, poorly organized interactions, while ordered hydrogen-bonded carbonyls correspond to urethane and urea groups engaged in strong, directional hydrogen bonding interactions, typically occurring within semi-crystalline domains. These interactions promote the formation of hard phases enriched in rigid segments stabilized by extensive intermolecular hydrogen bonding [36].

By integrating the areas under the deconvoluted carbonyl bands, the relative proportions of each carbonyl were quantified (see Figure 8c,d; Equation S4 and Table S11). Among these, the fraction of ordered hydrogen-bonded carbonyls, comprising both urethane and urea functionalities, can somewhat reflect the extent of microphase separation. This is based on the well-established correlation between the degree of hydrogen bond ordering and the organization of hard segments into phase-separated domains [36].

For **NIPU 1i**, the total relative fraction of ordered hydrogen-bonded carbonyls is 17.2%, whereas significantly higher values are observed for **NIPU 2** (48.8%) and **NIPU 3a** (52.6%). This marked increase in carbonyl ordering indicates a more pronounced organization of hard segments in **NIPUs 2** and **3a**, possibly consistent with the development of microphase-separated structures, and in good agreement with the presence of two thermal transitions as evidenced by DSC analyses.

Next, the thermal stability of the NIPUs was assessed using thermogravimetric analysis (TGA). The results are shown in Figure 9 and are summarized in Table 3. Aside from the minor volatilization of moisture below 200°C [9], two main degradation steps were identified by the derivative thermogravimetric analysis (DTG): the first step is observed in the DTG as a shoulder between 200°C and approximately 340°C and corresponds to the degradation of carbamate moieties leading to the generation of CO_2, alcohol, and amines [37–39]. This occurs first due to the lower thermal stability of carbamates in comparison to C–C bonds [21, 38, 40]. The second step, the prominent peak occurring between 340°C and >500°C, characterizes the main degradation due to the scission of the alkyl and ether groups [21, 38, 41, 42].

Considering the temperature corresponding to 5% of weight loss, $T_{d5\%}$, as a parameter for thermal stability, the NIPUs exhibit stability in the range of 226°C–299°C, comparable to that of aliphatic TPUs with polyether backbones [21, 40]. Variations in thermal stability are attributed to factors including the number of urethane groups and carbons in the repeat unity structure and the type of monomers incorporated [11, 41, 43]. For instance, in the case of **NIPU 1i**, the lowest density of carbamate groups leads to the highest thermal stability.

For the mechanical testing, **NIPU 1i** and **NIPU 2** were displaced in a metal dogbone-shaped mold, in which the samples were prepared using a hot press under a temperature of 120°C and a pressure of 4 bar for ~10 min. The materials were then submitted to a tensile test. The stress–strain curves of the NIPUs are presented in Figure 10 and Table 4, respectively. The analyzed NIPUs exhibited ductile behavior with a yield point and followed by a broad plastic deformation from ~50% up to 400–500% [34, 44]. This mechanical profile is typical of elastomeric semi-crystalline TPUs produced with isocyanates [34, 45]. **NIPU 1i** is the most rigid polymer with a Young's Modulus of $E = 107$ MPa and a tensile strength of $\sigma_b = 9.54$ MPa. These results are similar to those previously investigated using aliphatic diisocyanate and telechelic polyether polyol [45]. In contrast, **NIPU 2**, obtained from 1,5-pentanediol, exhibits lower values, with $E = 81$ MPa and $\sigma_b = 8.98$ MPa. The lower rigidity observed in **NIPU 2** is explained by the incorporation of an additional diol that negatively affects the polymer's crystallinity, as discussed previously (Table 3), and

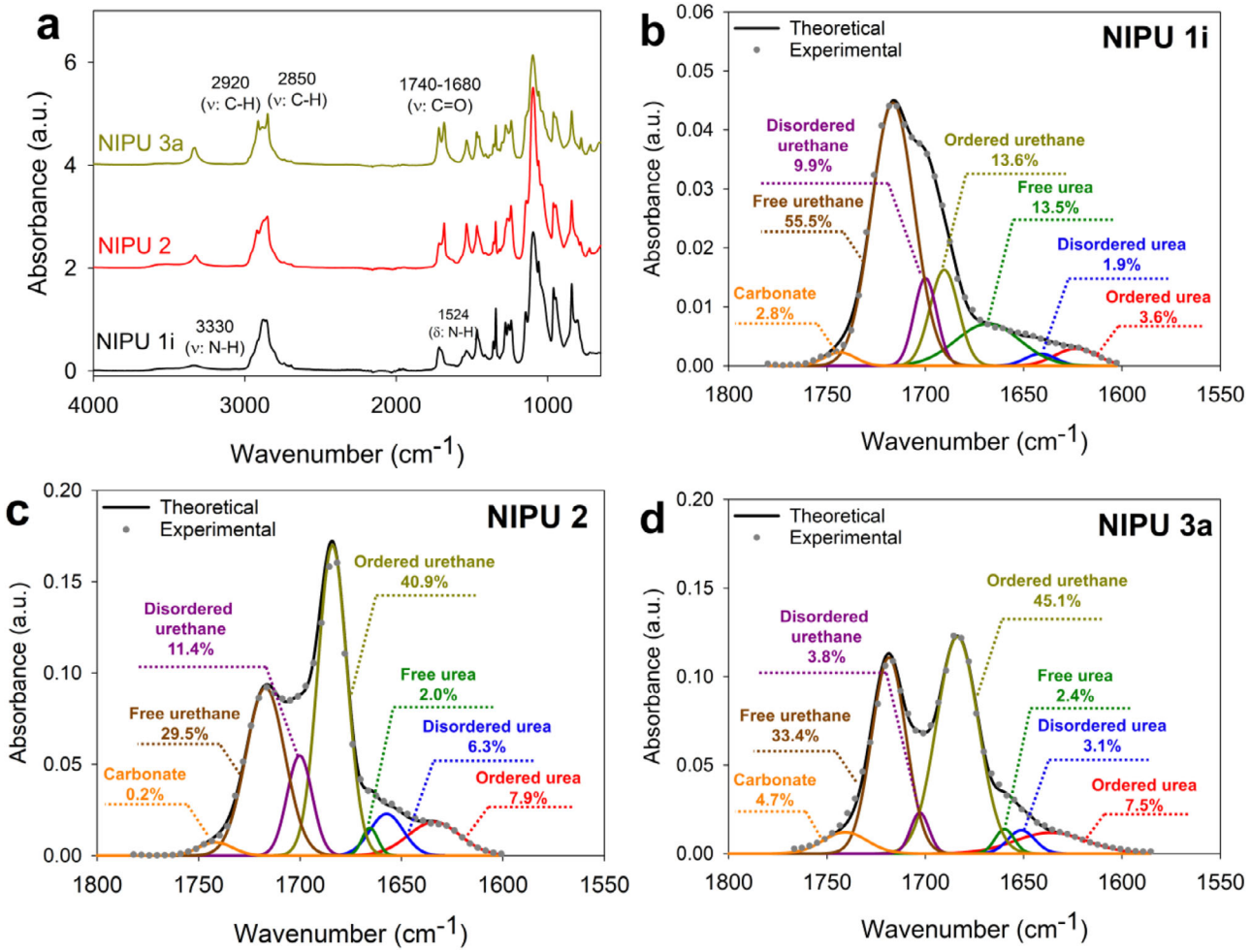

FIGURE 8 | (a) FTIR spectra of **NIPUs 1i, NIPU 2,** and NI**PU 3a** with peak deconvolution of the carbonyl stretching region for (b) **NIPU 1i**, (c) **NIPU 2**, (d) **PU 3a**.

TABLE 4 | Mechanical properties of **NIPU 1i** and **NIPU 2**.

	Young's Modulus, *E* [MPa]	**Tensile strength, σ_b [MPa]**	**Elongation at break, ε_b [%]**
NIPU 1i	107 ± 8	9.54 ± 0.63	235.26 ± 207.16
NIPU 2	81 ± 15	8.98 ± 0.91	152.39 ± 193.75

reduces the overall mechanical properties. Similar effect was observed in polyurethanes produced with dihydroxy telechelic polyester [32].

4 | Conclusion

Non-isocyanate polyurethanes were produced by transurethanization of dimethyl dodecane-1,12-diyldicarbamate (**3**) with dihydroxy telechelic polyethylene glycol (**4**) and different biobased diols. The transurethanization reaction was performed at a relatively low temperature (120°C) in comparison to other studies. Nevertheless, high NIPU molar masses (up to M_n = 94.3 kg × mol^{-1}) and relatively low urea content (4.9 mol%) could be achieved, in contrast to already published data. The high molar mass was accomplished as a result of the experimental condition optimization, revealing the benefit of mechanical stirring, use of KOtBu catalyst, and alcohol/carbamate ratio equal to 0.9.

Using the optimized method, NIPUs were synthesized via the transurethanization of dicarbamates with PEG and short alkyl diols in a one-shot process. Under these conditions, polymers with M_n of up to 74.3 kg × mol^{-1} were obtained. However, when targeting NIPUs with melting points above 120°C, the resulting polymers exhibited lower molar masses (M_n = 43.8 kg × mol^{-1}). To address this limitation, the reaction protocol was modified by introducing stepwise temperature adjustments at 135°C (~T_{m2}) and 150°C (>T_{m2}), which successfully increased M_n to 54.9 kg × mol^{-1}. These findings highlight the potential of the developed conditions for adapting the temperature profiles synthesis of

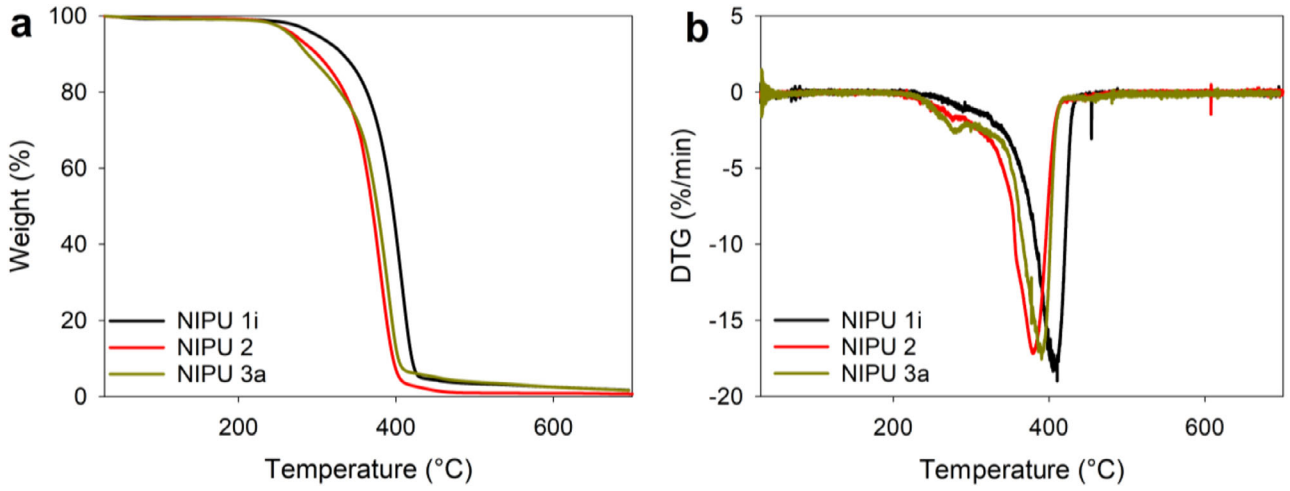

FIGURE 9 | (a) TGA and (b) DTG curves of **NIPUs 1–3**.

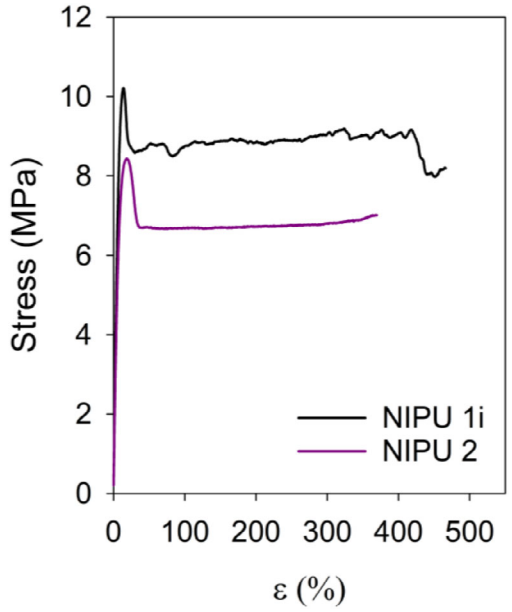

FIGURE 10 | Stress vs. strain curves of **NIPU 1i** and **NIPU 2**.

NIPUs with various diol mixtures, including volatile diols, while achieving high molar masses.

The thermal properties of the prepared NIPUs were assessed by TGA and DSC, revealing thermal stability higher than 220°C, thermal properties of typical semi-crystalline materials, and ductile mechanical behavior typical of TPUs.

Acknowledgements

The authors would like to express thanks for the financial support provided by the NIPU-EJD project; this project has received funding from the European Union's Horizon 2020 research and innovation program under Marie Skłodowska-Curie Grant Agreement No. 955700.

Conflicts of Interest

The authors declare no conflicts of interest.

Data Availability Statement

The data that support the findings of this study are available from the corresponding author upon reasonable request.

References

1. L. Maisonneuve, O. Lamarzelle, E. Rix, E. Grau, and H. Cramail, "Isocyanate-Free Routes to Polyurethanes and Poly(hydroxy Urethane)s," *Chemical Reviews* 115, no. 22 (2015): 12407–12439.

2. A. Llevot and M. A. R. Meier, "Perspective: Green Polyurethane Synthesis for Coating Applications," *Polymer International* 68, no. 5 (2019): 826–831.

3. M. Unverferth, O. Kreye, A. Prohammer, and M. A. R. Meier, "Renewable Non-Isocyanate Based Thermoplastic Polyurethanes via Polycondensation of Dimethyl Carbamate Monomers With Diols," *Macromolecular Rapid Communications* 34, no. 19 (2013): 1569–1574.

4. B. Bizet, E. Grau, J. M. Asua, and H. Cramail, "Hybrid Nonisocyanate Polyurethanes (H-NIPUs): A Pathway Towards a Broad Range of Novel Materials," *Macromolecular Chemistry and Physics* 223, no. 13 (2022): 2100437.

5. G. Coste, D. Berne, V. Ladmiral, C. Negrell, and S. Caillol, "Non-Isocyanate Polyurethane Foams Based on Six-Membered Cyclic Carbonates," *European Polymer Journal* 176 (2022): 111392.

6. M. Firdaus and M. Meier, "Renewable Polyamides and Polyurethanes Derived From Limonene," *Green Chemistry* 15, no. 2 (2013): 370–380.

7. S. Ma, H. Zhang, R. Sablong, C. Koning, and R. van Benthem, "t -Butyl-Oxycarbonylated Diamines as Building Blocks for Isocyanate-Free Polyurethane/Urea Dispersions and Coatings," *Macromolecular Rapid Communications* 39, no. 9 (2018): 1800004.

8. O. Kreye, S. Wald, and M. Meier, "Introducing Catalytic Lossen Rearrangements: Sustainable Access to Carbamates and Amines," *Advanced Synthesis & Catalysis* 355, no. 1 (2013): 81–86.

9. C. Duval, N. Kébir, A. Charvet, A. Martin, and F. Burel, "Synthesis and Properties of Renewable Nonisocyanate Polyurethanes (NIPUs) From Dimethylcarbonate," *Journal of Polymer Science Part A: Polymer Chemistry* 53, no. 11 (2015): 1351–1359.

10. S. Li, Y. Deng, J. Zhao, Z. Zhang, J. Zhang, and W. Yang, "Synthesis and Properties of Non-Isocyanate Crystallizable Aliphatic Thermoplastic

Polyurethanes," *Journal of Wuhan University of Technology-Mater Sci Ed* 33, no. 5 (2018): 1275–1280.

11. N. Kébir, M. Benoit, and F. Burel, "Elaboration of AA-BB and AB-type Non-Isocyanate Polyurethanes (NIPUs) Using a Cross Metathesis Polymerization Between Methyl Carbamate and Methyl Carbonate Groups," *European Polymer Journal* 107 (2018): 155–163.

12. I. Yilgör, E. Yilgör, and G. Wilkes, "Critical Parameters in Designing Segmented Polyurethanes and Their Effect on Morphology and Properties: A Comprehensive Review," *Polymer* 58 (2015): A1–A36.

13. B. Cheng, W. Gao, X. Ren, et al., "A Review of Microphase Separation of Polyurethane: Characterization and Applications," *Polymer Testing* 107 (2022): 107489.

14. L. Korley, B. Pate, E. Thomas, and P. Hammond, "Effect of the Degree of Soft and Hard Segment Ordering on the Morphology and Mechanical Behavior of Semicrystalline Segmented Polyurethanes," *Polymer* 47, no. 9 (2006): 3073–3082.

15. Y. Jung, S. Lee, J. Park, and E. Shin, "One-Shot Synthesis of Thermoplastic Polyurethane Based on Bio-Polyol (Polytrimethylene Ether Glycol) and Characterization of Micro-Phase Separation," *Polymers* 14, no. 20 (2022): 4269.

16. Z. Shen, J. Zhang, W. Zhu, et al., "A Solvent-Free Route to Non-Isocyanate Poly(Carbonate Urethane) With High Molecular Weight and Competitive Mechanical Properties," *European Polymer Journal* 107 (2018): 258–266.

17. N. Jaques, A. Llevot, É. Grau, T. Vidil, M. Meier, and H. Cramail, "High Molar Mass Non-Isocyanate Polyurethanes by Transurethanization of Diols With Isophorone-Based Bismethylcarbamate," *Macromolecular Chemistry And Physics* 226 (2025): 2500068.

18. D. Wolosz, P. Parzuchowski, and A. Swiderska, "Synthesis and Characterization of the Non-Isocyanate Poly(Carbonate-Urethane)s Obtained via Polycondensation Route," *European Polymer Journal* 155 (2021): 110574.

19. S. Ye, X. Xiang, S. Wang, D. Han, M. Xiao, and Y. Meng, "Non-isocyanate CO_2-Based Poly(Ester-Co-Urethane)s With Tunable Performances: A Potential Alternative to Improve the Biodegradability of PBAT," *ACS Sustainable Chemistry & Engineering* 8, no. 4 (2020): 1923–1932.

20. Z. Shen, L. Zheng, C. Li, et al., "A Comparison of Non-Isocyanate and HDI-Based Poly(Ether Urethane): Structure and Properties," *Polymer* 175 (2019): 186–194.

21. N. Kebir, S. Nouigues, P. Moranne, and F. Burel, "Nonisocyanate Thermoplastic Polyurethane Elastomers Based on Poly(Ethylene Glycol) Prepared Through the Transurethanization Approach," *Journal of Applied Polymer Science* 134, no. 45 (2017): 44991.

22. J. Qin, J. Jiang, S. Ye, et al., "High Performance Poly(Urethane-Co-Amide) From CO_2-Based Dicarbamate: An Alternative to Long Chain Polyamide," *RSC Advances* 9, no. 45 (2019): 26080–26090.

23. Z. Shen, L. Zheng, D. Song, et al., "A Non-Isocyanate Route to Poly(Ether Urethane): Synthesis and Effect of Chemical Structures of Hard Segment," *Polymers* 14, no. 10 (2022): 2039.

24. F. Magliozzi, G. Chollet, E. Grau, and H. Cramail, "Benefit of the Reactive Extrusion in the Course of Polyhydroxyurethanes Synthesis by Aminolysis of Cyclic Carbonates," *ACS Sustainable Chemistry & Engineering* 7, no. 20 (2019): 17282–17292.

25. S. Ma, C. Liu, R. Sablong, et al., "Catalysts for Isocyanate-Free Polyurea Synthesis: Mechanism and Application," *ACS Catalysis* 6, no. 10 (2016): 6883–6891.

26. S. Bruniaux, R. Varma, and C. Len, "A Novel Strategy for Selective O-Methylation of Glycerol in Subcritical Methanol," *Frontiers in Chemistry* 7 (2019): 357.

27. G. Rokicki and A. Piotrowska, "A New Route to Polyurethanes From Ethylene Carbonate, Diamines, and Diols," *Polymer* 43, no. 10 (2002): 2927–2935.

28. Y. Deng, S. Li, J. Zhao, Z. Zhang, J. Zhang, and W. Yang, "Aliphatic Thermoplastic Poly(Ether Urethane)s Having Long PEG Sequences Synthesized Through a Non-Isocyanate Route," *Chinese Journal of Polymer Science* 33, no. 6 (2015): 880–889.

29. D. Visser, H. Bakhshi, K. Rogg, et al., "Green Chemistry for Biomimetic Materials: Synthesis and Electrospinning of High-Molecular-Weight Polycarbonate-Based Nonisocyanate Polyurethanes," *ACS Omega* 7 (2022): 39772–39781.

30. P. Dongdon and T. Hengshui, "Polycarbonate Polyurethane Elastomers Synthesized via a Solvent-Free and Nonisocyanate Melt Transesterification Process," *Journal of Applied Polymer Science* 132, no. 7 (2015): 41377.

31. X. Zhao, T. Shou, R. Liang, S. Hu, P. Yu, and L. Zhang, "Bio-Based Thermoplastic Polyurethane Derived From Polylactic Acid With High-Damping Performance," *Industrial Crops and Products* 154 (2020): 112619.

32. T. Calvo-Correas, M. Martin, A. Retegi, N. Gabilondo, M. Corcuera, and A. Eceiza, "Synthesis and Characterization of Polyurethanes with High Renewable Carbon Content and Tailored Properties," *ACS Sustainable Chemistry & Engineering* 4, no. 10 (2016): 5684–5692.

33. S. Li, Z. Sang, J. Zhao, Z. Zhang, J. Zhang, and W. Yang, "Crystallizable and Tough Aliphatic Thermoplastic Polyureas Synthesized through a Nonisocyanate Route," *Industrial & Engineering Chemistry Research* 55, no. 7 (2016): 1902–1911.

34. R. Waletzko, L. Korley, B. Pate, E. Thomas, and P. Hammond, "Role of Increased Crystallinity in Deformation-Induced Structure of Segmented Thermoplastic Polyurethane Elastomers With PEO and PEO−PPO−PEO Soft Segments and HDI Hard Segments," *Macromolecules* 42, no. 6 (2009): 2041–2053.

35. A. Niemczyk, A. Piegat, A. Olalla, and M. El Fray, "New Approach to Evaluate Microphase Separation in Segmented Polyurethanes Containing Carbonate Macrodiol," *European Polymer Journal* 93 (2017): 182–191.

36. D. Xiang, M. Liu, G. Chen, T. Zhang, L. Liu, and Y. Liang, "Optimization of Mechanical and Dielectric Properties of Poly (Urethane–Urea) -Based Dielectric Elastomers via the Control of Microstructure," *RSC Advances* 7, no. 88 (2017): 55610–55619.

37. L. Yinlei, H. Deliu, H. Huawen, et al., "Preparation and Properties of Polydimethylsiloxane (PDMS)/Polyethylene Glycol (PEG)-Based Amphiphilic Polyurethane Elastomers," *ACS Applied Bio Materials* 2, no. 10 (2019): 4377–4384.

38. P. Boisaubert, N. Kébir, A. Schuller, and F. Burel, "Polyurethane Coatings From Formulations With Low Isocyanate Content Using a Transurethane Polycondensation Route," *Polymer* 240 (2022): 124522.

39. P. Parcheta, E. Glowinska, and J. Datta, "Effect of Bio-Based Components on the Chemical Structure, Thermal Stability and Mechanical Properties of Green Thermoplastic Polyurethane Elastomers," *European Polymer Journal* 123 (2020): 109422.

40. S. Li, J. Zhao, Z. Zhang, J. Zhang, and W. Yang, "Synthesis and Characterization of Aliphatic Thermoplastic Poly(Ether Urethane) Elastomers Through a Non-Isocyanate Route," *Polymer* 57 (2015): 164–172.

41. W. Lei, C. Fang, X. Zhou, Y. Cheng, R. Yang, and D. Liu, "Morphology and Thermal Properties of Polyurethane Elastomer Based on Representative Structural Chain Extenders," *Thermochimica Acta* 653 (2017): 116–125.

42. A. More, T. Lebarbé, L. Maisonneuve, B. Gadenne, C. Alfos, and H. Cramail, "Novel Fatty Acid Based Di-Isocyanates Towards the Synthesis of Thermoplastic Polyurethanes," *European Polymer Journal* 49, no. 4 (2013): 823–833.

43. S. Oprea, D. Timpu, and V. Oprea, "Design-Properties Relationships of Polyurethanes Elastomers Depending on Different Chain Extenders Structures," *Journal Of Polymer Research* 26, no. 5 (2019): 117.

44. D. Wołosz and P. G. Parzuchowski, "Biobased Non-Isocyanate Poly(Carbonate-Urethane)s of Exceptional Strength and Flexibility," *Polymer* 254 (2022): 125026.

45. M. Rogulska, A. Kultys, and E. Olszewska, "New Thermoplastic Poly(Thiourethane-Urethane) Elastomers Based on Hexane-1,6-diyl Diisocyanate (HDI)," *Journal of Thermal Analysis and Calorimetry* 114, no. 2 (2013): 903–916.

Supporting Information

Additional supporting information can be found online in the Supporting Information section.

Supporting file: macp70084-sup-0001-SuppMat.docx